Available online at www.sciencedirect.com
SCIENCE DIRECT®
Polymer 45 (2004) 49–59
polymer
www.elsevier.com/locate/polymer

Structure of poly (*p*-phenylenebenzobisoxazole) (PBZO) and poly (*p*-phenylenebenzobisthiazole) (PBZT) for proton exchange membranes (PEMs) in fuel cells

Soo-Young Park[a], Hilmar Koerner[b], S. Putthanarat[c], Rahmi Ozisik[d], Shane Juhl[e], B.L. Farmer[e], R.K. Eby[c,*]

[a]*Department of Polymer Science, Kyungpook National University, Daegu 702-701, South Korea*
[b]*Nonmetallic Materials Division, University of Dayton Research Institute, 300 College Park Ave, Dayton, OH 45469-0168, USA*
[c]*Department and Institute of Polymer Science, The University of Akron, 170 University Avenue, Akron, OH 44325-3909, USA*
[d]*Department of Materials Science and Engineering, MRC 205, Rensselaer Polytechnic Institute, Troy, NY 12180-3590, USA*
[e]*Air Force Research Laboratory, AFRL/MLBP, Wright-Patterson AFB, OH 45433-7750, USA*

Received 14 July 2003; received in revised form 7 October 2003; accepted 9 October 2003

Abstract

The structures of membranes of PBZO and PBZT extruded with counter rotating dies (CRD) were studied by wide angle X-ray diffraction (WAXD), small angle X-ray scattering (SAXS), atomic force, scanning electron and transmission electron microscopy (AFM, SEM, and TEM). The structure of CRD-extruded PBZO was compared with that of a solution-cast membrane. The extruded membranes have sheet structures typical of rigid-rod polymers. The heterocyclic rings of the extruded membranes are oriented approximately parallel to the membrane surface, while those of the cast membrane are oriented perpendicular to the surface. The parallel orientation of the rings of the extruded membranes may be due to the normal force exerted during extrusion. The polymer molecules near the surfaces of the extruded membranes are oriented along the shear directions of the extruder, while those in the middle are oriented randomly. There is little cholesteric nature. These materials have potential as microporous PEMs holding ion conducting polymers (ICPs).

Keywords: PBZO; PBZT; PEMs

1. Introduction

In the present polymer electrolyte fuel cells, PEMs employ extensively fluorinated ion conducting polymers ((ICPs) such as Nafion®) that have specific limitations [1,2]. These include poor ion conductivities at low humidities and/or elevated temperatures, susceptibility to chemical degradation at elevated temperatures, and membrane cost. Microcomposite PEMs employing a high strength, chemically inert, and high temperature material as a supporting membrane for containing ICPs appear to be a promising approach to overcoming the cost/performance shortcomings of current PEM technology [3,4]. The membrane substrate should contain flow channels for the ICP that transports protons from the fuel cell's anode to cathode. As supporting substrates, rigid-rod polymers such as PBZO and PBZT have the potential to meet the requirements for improved PEMs. Advantages of rigid-rod polymers are high strength (0.69 GPa), dimensional stability, chemical resistance, good barrier properties, good high temperature properties providing increased fuel cell efficiency, and a tailorable open structure accommodating varied ICP loadings [5,6]. This article reports on the structure and morphology of (CRD) extruded PBZO and PBZT membranes determined with wide angle X-ray diffraction (WAXD), small angle X-ray scattering (SAXS), SEM, TEM and AFM. Some information is given on a cast PBZO membrane.

Fratini et al. reported the crystal structure of PBZO in which two molecules pass through a monoclinic unit cell [7]. A prominent characteristic is the axial disorder in the crystal, which causes streaks along the layer lines in the fiber pattern [8]. Martin et al. proposed a disordered

* Corresponding author. Tel.: +1-330-972-5397; fax: +1-330-972-6581.
E-mail address: reby@uakron.edu (R.K. Eby).

0032-3861/$ - see front matter © 2003 Elsevier Ltd. All rights reserved.
doi:10.1016/j.polymer.2003.10.033

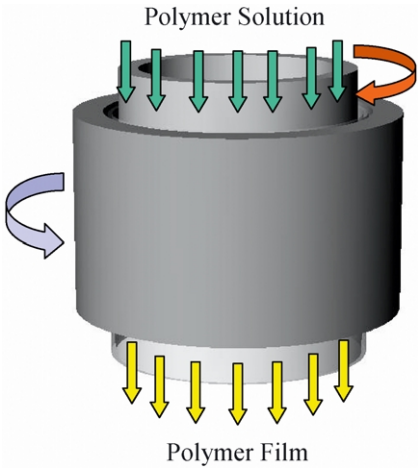

Fig. 1. Schematic diagram of a CRD.

structure in which the neighboring molecules of PBZO are randomly shifted side by side by $\pm c/4$ along the *a*-axis [8]. Tashiro et al. studied the crystal structure and packing disorder of PBZO using computer simulation [9]. The molecules form layers extending along the *110* planes with the relative heights of the adjacent molecules in the sheets almost confined to either $+c/4$ or $-c/4$ and these sheets are stacked together in the *b*-axis direction with random heights along the molecular axis. Fratini et al. gave the structure of the monoclinic unit cell for PBZT [7]. Takahashi et al. proposed that the molecular heights are disordered by 1/2 on the *ac* plane and by 1/5 on the *bc* plane [10]. The cell parameters and schematic structures for PBZO and PBZT are summarized elsewhere [11].

Rigid-rod polymers are normally fabricated into thin membranes by two methods: casting from dilute solution (~1–2 wt%) and uniaxial extrusion from a concentrated solution in the nematic state (~5–10 wt%). In the casting process, a uniform membrane is cast by using a doctor blade with a spacer for a certain thickness. High concentration polymer dopes (in the isotropic state) are difficult to process due to the high viscosity of the solution. Viscosity in the isotropic state exponentially increases with concentration of the solution. Thus, generally a low concentration of the solution is necessary. However, membranes made from low concentration often exhibit weak mechanical properties. In order to get good mechanical properties, extrusion of nematic solutions must be employed. The uniaxial membrane extrusion process yields a highly oriented membrane [12] for which weak transverse properties can be expected especially for rigid-rod polymers because of the high anisotropy of the molecules in the nematic solution. Foster–Miller, Inc. developed a method for producing biaxially-oriented membranes using a CRD system [13]. In CRD extrusion, the material is extruded between two concentric counter-rotating coaxial cylinders (dies) (Fig. 1). Therefore, the net shear on the cylindrical extrudate's inner and outer surfaces are the vector sums of the machine direction shear imparted by the extrusion itself, and the transverse shears imparted by the counter rotation of the dies' cylinder barrels. Thus, the molecular orientation with respect to the machine direction will be plus theta on one surface of the membrane and minus theta on the other (theta is the angle between the machine and shear directions). In the present work, theta is typically ~22 degrees. Thus, the molecules on the membrane surface can be easily oriented along the shear direction of the CRD-extruder. However, the orientation in the interior part of the membrane has not been explored. The molecular directors may go through a cholesteric twist from minus theta to plus theta, with the orientation in the middle of the membrane's thickness being about 0 degrees with respect to machine direction. Another possibility is that molecules in the middle part of the membrane are randomly oriented while the molecules closer to the surfaces are oriented along the shear directions.

2. Experimental

2.1. Materials

Cast PBZO membranes were produced from 1% PBZO solution in methyl sulfonic acid (MSA). The membranes were coagulated in phosphoric acid (H_3PO_4) and water successively. CRD-extruded membranes were produced from 14% PBZO solution in polyphosphoric acid (PPA) and coagulated in water immediately after extrusion. PBZT membranes were CRD-extruded in a similar manner. All the membranes were dried at 255 °C in a tension ring.

2.2. X-Ray

WAXD patterns were recorded under vacuum on phosphor image plates (Molecular Dynamics©) in a Warhus camera. Ni filtered Cu radiation from a rotating anode X-ray generator operating at 40 kV and 150 mA was used. The sample to detector distance of 53 mm was calibrated with SiO_2 powder. 2D SAXS experiments were conducted on the synchrotron X-ray beamline X27C at Brookhaven National Laboratory. The wavelength of the X-ray beam was 0.1366 nm with a sample to detector distance of 1350 mm keeping most of the beam path under vacuum. The beam was collimated with a three pinhole system to allow resolutions of up to 1000 Å at a beam spot diameter of 0.1 mm. Additional scattering by air was subtracted before analysis. All experiments were conducted at room temperature. X-ray patterns were collected on a 2D MAR CCD detector. Both WAXD and SAXS patterns were analyzed using the public domain software package Fit2D [14] as well as the reported structures in conjunction with the Cerius^2 4.6 software produced by Accelrys, San Diego, CA [7,8,11].

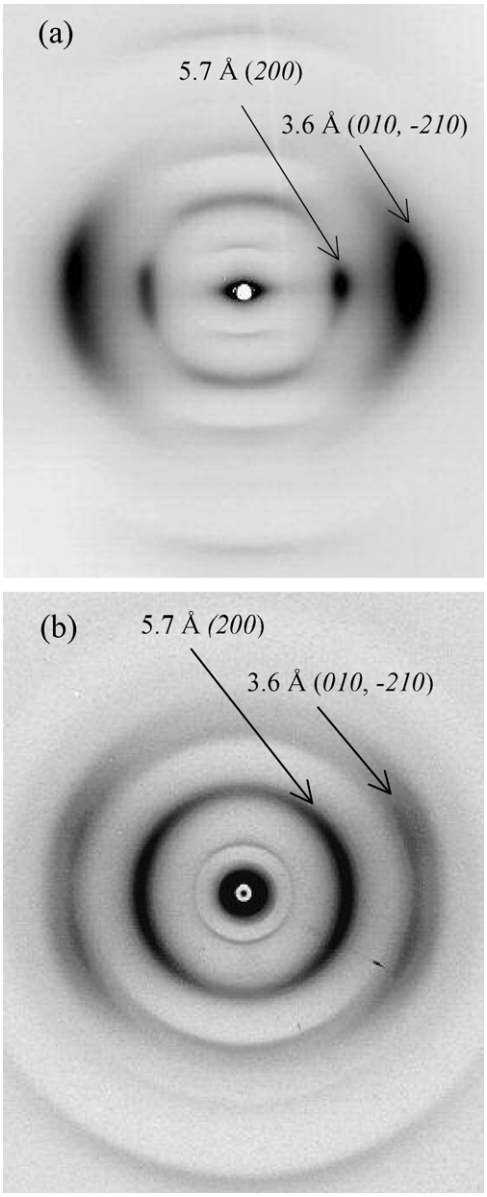

Fig. 2. WAXD patterns of the CRD-extruded PBZO membrane with the X-ray beam (a) parallel to the membrane surface (vertical is the machine direction) and (b) perpendicular to the membrane surface (horizontal is the machine direction).

2.3. Microscopy

For higher resolution images, Hitachi S-900 and S-4700 low voltage high resolution SEMs were used. Fracture surfaces were prepared by immersing the membranes in liquid nitrogen prior to fracture. TEM images were obtained using a Philips CM-200 TEM. The samples suitable for TEM were microtomed from an epoxy mounted sample. The membrane surface was etched with oxygen plasma, which was generated using a GSC-200 plasma generator (March Instruments, Inc. Concord CA). The oxygen concentration was ~1018 ions (or radicals) per liter. An optical lever type atomic force microscope (AFM), TopoMetrix 2010, was used in the repulsive contact mode at ambient conditions. Small pieces of the membranes were mounted on the sample holder with double-sided tape. Layers were peeled from both surfaces of the membrane with Scotch® tape. The peeling of each layer was accompanied with an AFM analysis to measure the thickness of the peeled layer, and to characterize the newly uncovered underlying surface. Images were obtained with a constant force of $\sim 10^{-10}$–10^{-9}N. Cantilevers with a silicon nitride tip of ~50 nm radius were used. The scanning frequency was 0.15–2 Hz with 200–400 data points being taken on each of the scan lines.

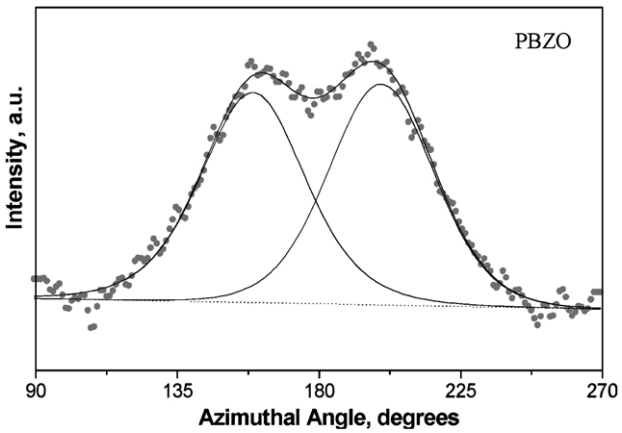

Fig. 3. Azimuthal scan of the reflection at $d = 3.6$ Å of Fig. 2(b) and its curve resolution with Gaussian profiles (the machine direction is 180 degrees).

3. Results and discussion

3.1. WAXD results

3.1.1. PBZO

Fig. 2(a) shows the WAXD pattern of the CRD-extruded PBZO membrane with the X-ray beam parallel to the membrane surface (transverse direction, td). A series of reflections with orders of $d = 12.1$ Å are parallel to the membrane surface. Two strong reflections at $d = 5.7$ and 3.6 Å are nearly perpendicular to the membrane surface. The d-spacing values and locations of the series of reflections with orders of $d = 12.1$ Å indicate that they are *00l* reflections and the molecules are approximately parallel to the membrane surface. The reflection at $d = 5.7$ Å is *200* and represents the approximately side-by-side packing of the ring structures. The second reflection at $d = 3.6$ Å contains two reflections of *010* and -210 and represents the face-to-face packing of the ring structures. Fig. 2(b) shows the WAXD pattern with the X-ray beam perpendicular to the membrane surface (normal direction, nd). The same reflections as in Fig. 2(a) are observed in terms of d-spacing while their relative intensities and orientations changed. Fig. 3 shows the azimuthal scan of the reflection at $d = 3.6$ Å of

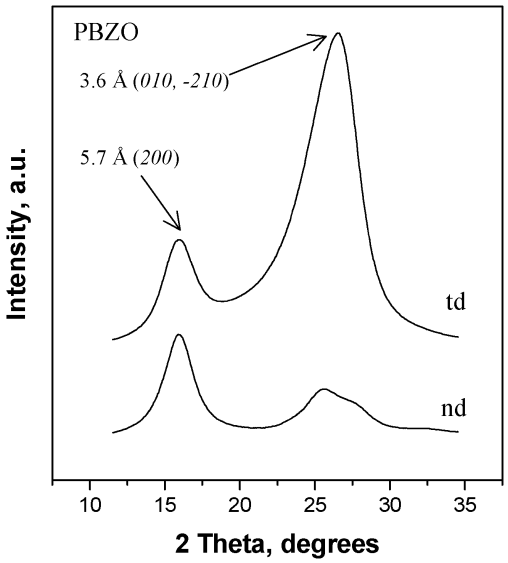

Fig. 4. Intensity profile along the horizontal direction in Fig. 2(a) and (b).

Fig. 2(b). The reflection comprises two peaks separated by ~40 degrees, which is the angle between the shear directions on the outside and inside surfaces of the membrane (~ ± 20 degrees with respect to the machine direction) in the CRD extrusion (The 'outside surface' is the one against the outer rotating die and the 'inside surface' is against the inner die). This result suggests that the molecules on the outside and inside surfaces are oriented along the shear directions. As will be seen below, these results agree approximately with data from AFM and SAXS.

Next, we are interested in the molecular orientation in the middle part of the membrane. Rheological calculations need to be made to know the direction of the shear flow within the membrane during the CRD extrusion and they are beyond the scope of the present research. One possible manner of orientation is through a cholesteric twist from ~ − 20 degrees to ~ + 20 degrees, with the orientation in the middle of the membrane's thickness being about 0 degrees with respect to machine direction. The intensity along the azimuthal direction represents the population of the molecules oriented in the azimuthal direction. If the molecules were oriented in a cholesteric twist with equal population of molecular directors from ~ − 20 degrees to ~ + 20 degrees along the thickness direction, the intensity would be uniform along the azimuthal angle between those angles. Thus, observance of maximum intensity at ~ ± 20 degrees indicates that the populations oriented at ~ ± 20 degrees are denser than the populations oriented at other angles. The most likely molecular orientation to match the X-ray pattern is that the molecules on the outside and inside of the membrane are oriented along the shear directions while the molecules in the middle part of the membrane are oriented randomly. The detailed molecular orientation will be discussed with the AFM and SEM results.

Fig. 4 shows the intensity profile along the horizontal direction in Fig. 2(a) and (b). It was obtained by integrating

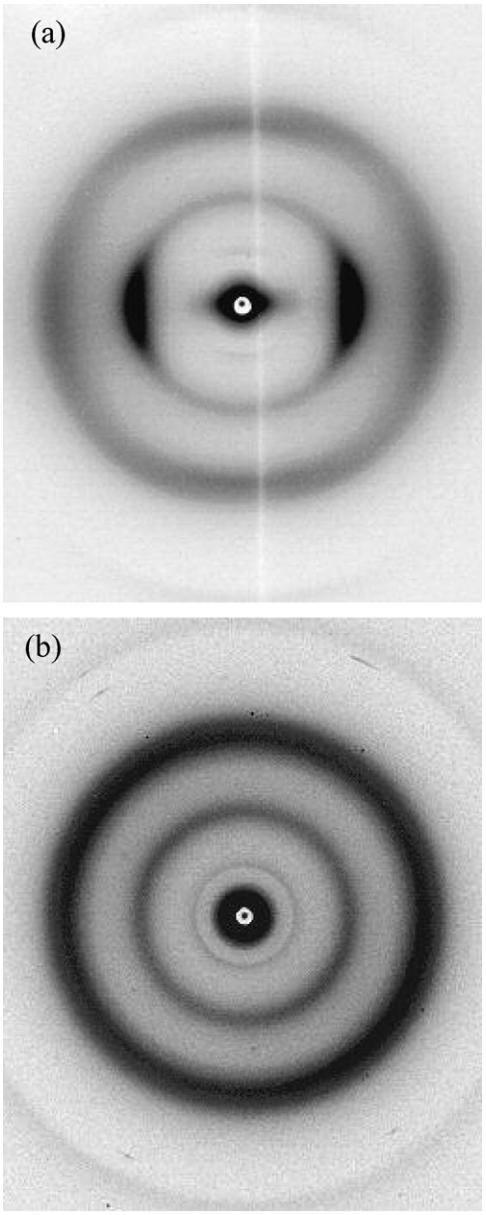

Fig. 5. WAXD patterns of the cast membrane PBZO with the X-ray beam (a) parallel and (b) perpendicular to the membrane surface.

along the azimuth from 110 to 250 degrees for the 2θ range from 11 to 34 degrees. The intensity of the second reflection at $d = 3.6$ Å $(010, -210)$ is stronger than that of the first reflection at $d = 5.7$ Å (200) when the X-ray beam is parallel to the membrane surface (td), while the intensity of the first reflection at $d = 5.7$ Å (200) is stronger than that of the second reflection $d = 3.6$ Å $(010, -210)$ when the X-ray beam is perpendicular to the membrane surface (nd). This relative intensity difference is due to the existence of planar orientation in the membrane. The ring planes are known to be approximately parallel to the -210 plane. The fact that the intensity of the -210 reflection became weak compared to that of the 200 reflection when the X-ray beam is perpendicular to the membrane surface suggests that

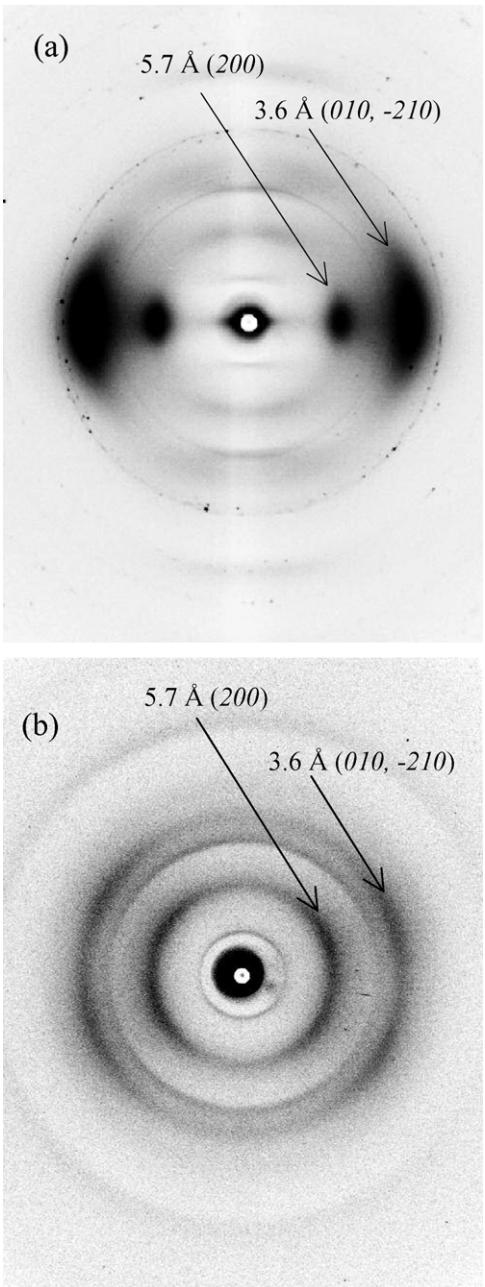

Fig. 6. Wide angle X-ray patterns of the CRD-extruded PBZT membrane with (a) the X-ray beam parallel to (vertical is approximately the machine direction) and (b) perpendicular to the membrane surface (horizontal is approximately the machine direction). The spotted ring in (a) is from the calibration standard.

heterocyclic rings are oriented approximately parallel to the membrane surface.

Fig. 5 shows the WAXD patterns of the cast PBZO membrane with the X-ray beam parallel (a) and perpendicular (b) to the surface. The same reflections as those from CRD-extruded membrane in terms of *d*-spacings were observed with different orientations and different relative intensities. Several isotropic rings were observed when the X-ray beam was perpendicular to the membrane surface (nd) and these were broken into arcs when the X-ray beam

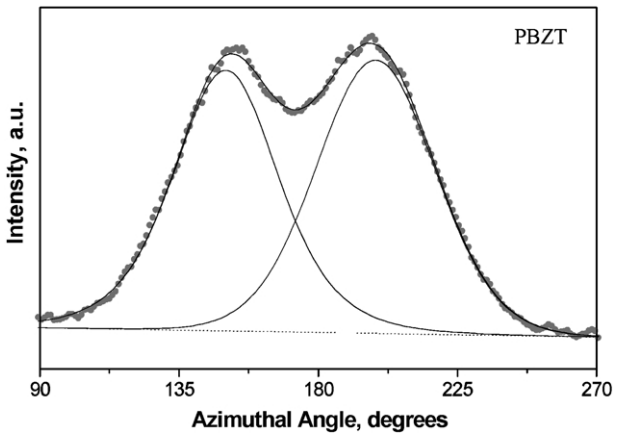

Fig. 7. Azimuthal scan of the reflection at $d = 3.6$ Å of Fig. 6(b) and its resolution with Gaussian profiles (the machine direction is approximately 180 degrees).

was parallel to the membrane surface (td). The anisotropy of the WAXD patterns indicates that there is a uni-planar (preferred planar) orientation in the cast membrane. Interestingly, the relative intensity difference of *200* and *−210* reflections is quite opposite to that of the CRD-extruded membrane. In the case of cast membrane, the *200* reflection is stronger than the *−210* reflection when the X-ray beam is parallel to the membrane surface, while the *200* reflection becomes weaker than the *−210* reflection when the X-ray beam is perpendicular to the membrane surface. This result strongly indicates that ring structures in the cast membrane are perpendicular to the membrane surface, unlike those in the CRD-extruded membrane. From the studies of other rigid-rod polymers such as PBZT and poly[(7-oxo-7H, 10H-benz(d,e)imidazo (4′,5′:5,6)-benzimidazo(2,1-a)isoquinoline-3,4:10,11-tetrayl)-10-carbonyl] (BBL), which were made with the casting method,

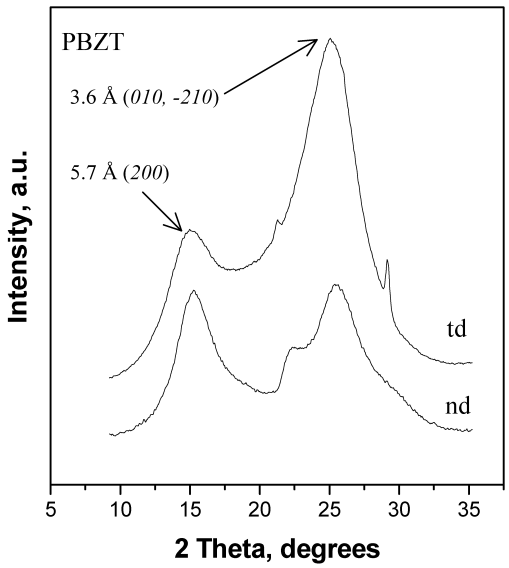

Fig. 8. Intensity profile along the horizontal direction in Fig. 6(a) and (b). The sharp peak at ~30 degrees is from an inorganic calibration standard.

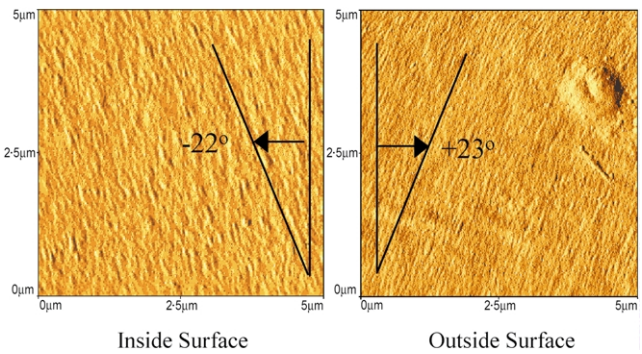

Fig. 9. AFM images of the inside and outside surfaces of the PBZO membrane. The machine direction is vertical and the images are 5 μm by 5 μm. See text.

heterocyclic rings are known to be oriented perpendicular to the membrane surface [15–17]. We found a quite different orientation of ring structures between the cast and extruded membranes. The reason why ring planes are oriented parallel to the membrane surface in the case of the CRD-extruded membrane may be that the normal force exerted on the membrane surface during extrusion, causes the large ring planes to be oriented nearly parallel to the membrane surface. Thus, the processing technique produces effects on the molecular level orientation.

3.1.2. PBZT

Similar WAXD patterns were taken with the CRD-extruded PBZT membrane. Fig. 6(a) is the pattern taken with the X-ray beam parallel to the membrane surface (td). A series of reflections with orders of ~12.5 Å are parallel to the membrane surface and the strong reflections at 5.7 Å (*200*) and 3.6 Å (*010*, −*210*) are nearly perpendicular to the surface. The *d*-spacing values and locations of the series of reflections with orders of $d = 12.5$ Å indicate that these are *001* reflections and that the molecules are nearly parallel to the membrane surface. The reflection at 5.7 Å is *200* and represents the approximate side by side packing of the ring structure. The reflection at 3.6 Å contains the *010* and −*210* reflections and represents the face to face packing of the benzobisthiazole and phenyl rings which are torsioned more with respect to one another than in PBZO [7,11]. Fig. 6(b) is the pattern taken with the beam perpendicular to the membrane surface (nd). The same reflections as in Fig. 6(a) can be observed, but their relative intensitites and orientations are changed. As in the case of PBZO in Fig. 2(b), the reflection at $d = 3.6$ Å clearly indicates the presence of two peaks. Fig. 7 shows the azimuthal scan of that reflection in Fig. 6(b). The angle between the two peaks is ~48 degrees indicating a maximum in the populations of the molecules at $\sim \pm 24$ degrees with respect to the machine direction. As will be seen below, this result agrees approximately with data from AFM and SAXS.

Fig. 8 shows the intensity profiles along the horizontal direction in Fig. 6(a) and (b). These were obtained in the same manner as were those in Fig. 4. The intensity of the second reflection at $d = 3.6$ Å (*010*, −*210*) is stronger than that of the first reflection at $d = 5.7$ Å (200) when the X-ray

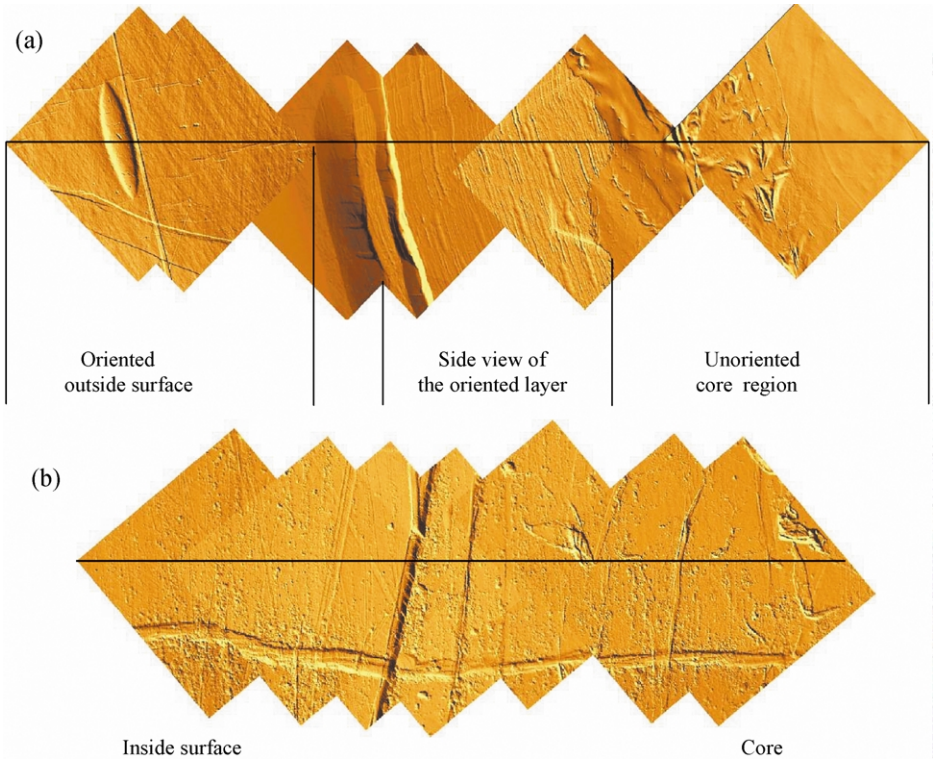

Fig. 10. Composite AFM image of the PBZO membrane after peeling (a) the outside surface and (b) the inside surface. The individual images are 70 μm by 70 μm.

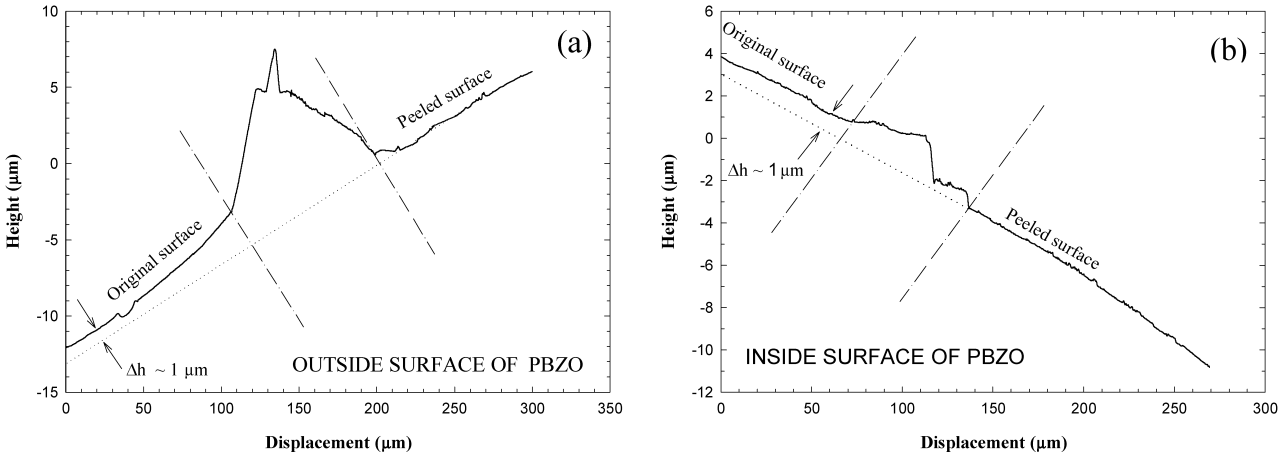

Fig. 11. Height profiles along the lines through the images in Fig. 10 (a) outside surface and (b) inside surface. Δh represents the thickness of the peeled skin layer.

beam is parallel to the membrane surface (td), but the intensity of the second reflection is relatively weaker when the beam is perpendicular to the membrane surface (nd). Since the rings in the molecular structure are approximately parallel to the (*010*) and (*−210*) planes, the results indicate that the rings are approximately parallel to the membrane surface. Again this might result from the normal force on the membrane during extrusion.

3.2. AFM results

3.2.1. PBZO

Fig. 9 shows AFM images of the inside and outside surfaces (as defined previously) of the PBZO membrane. The machine direction is vertical. The fibrils which can be seen are rotated approximately −22 and +23 degrees, respectively, from the machine direction. The inside surface was obtained by peeling multiple layers from the outside surface into the membrane. The last layer left on the double sided tape (on which the sample had been mounted for the AFM) was that of the inside layer. Scanning that layer makes it possible to view the correct relative orientation of the fibrils on the inside surface. That is, without the artificial orientation reversal that would occur if the whole membrane were simply turned over and scanned. The total angular separation based on 40 measurements is ~44 ± 4 degrees which agrees approximately with the value of 40 degrees determined by WAXD. More often, the PBZO membrane

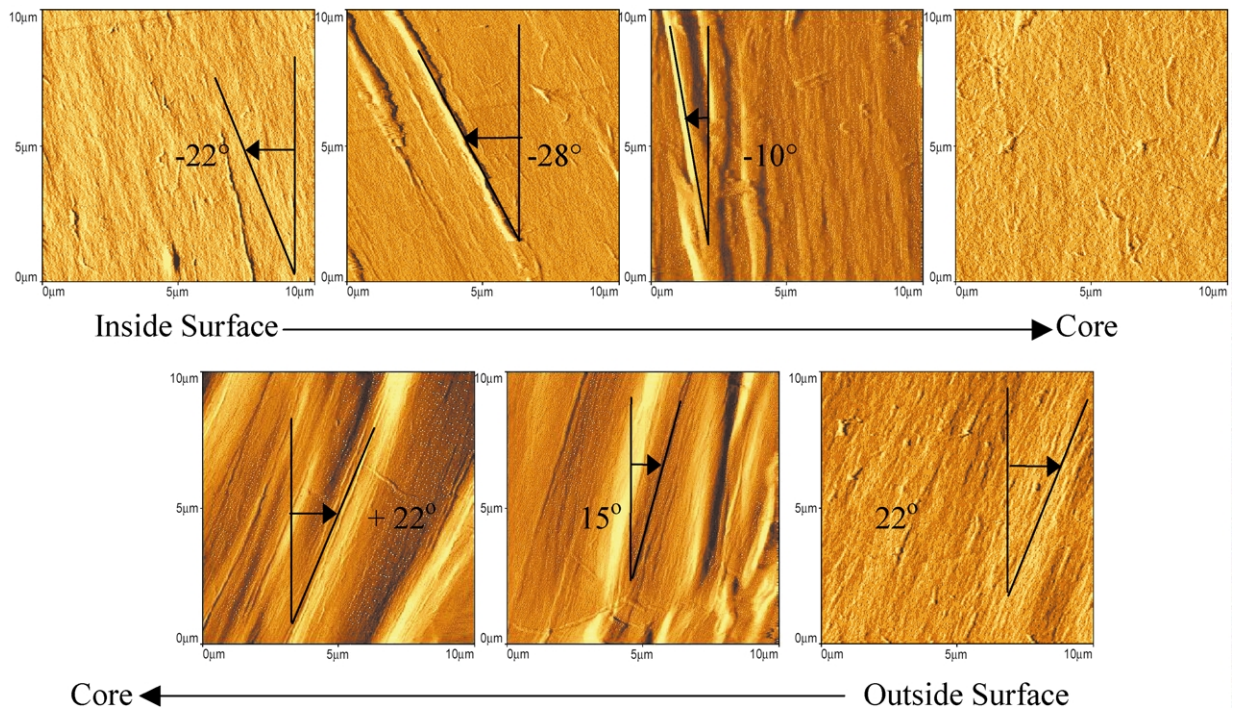

Fig. 12. A partial series of AFM images of surfaces exposed as the PBZT membranes was peeled. The images are 10 μm by 10 μm.

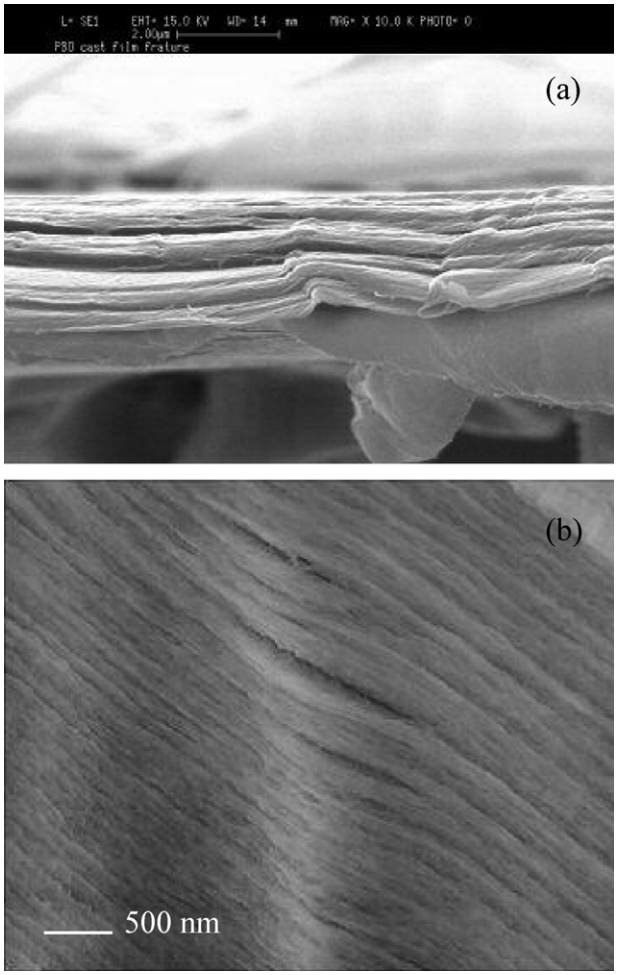

Fig. 13. Images of the CRD extruded PBZO membrane (a) SEM image of the fractured surface. (b) TEM image of a section microtomed perpendicular to the membrane surface.

did not peel in multiple layers. Fig. 10(a) shows a composite AFM image of the surface exposed by peeling the outside surface. The sample peeled in a thick section encompassing the outside surface to the core. In the middle of the peel the sample pulled up, but did not detach. The original oriented outside skin can be observed to the left and the unoriented irregular structure of the exposed core to the right. Fig. 10(b) shows the analogous data for the inside surface of the membrane. Fig. 11(a) and (b) show the height profiles along the lines through the images in Fig. 10(a) and (b). By extrapolating the exposed core profile to the area of the original surface, one can obtain an estimate of the thickness of the oriented layer on the outside and inside surfaces to be ~1 μm thick in the ~6.4 μm membrane. Thus, the PBZO membrane is about 70% core.

3.2.2. PBZT

The PBZT membrane exhibited a similar morphology with little cholerestic nature. It could be peeled in consecutive layers about 100 nm thick. In the peeled layers, the orientation of the fibrils fluctuated randomly in

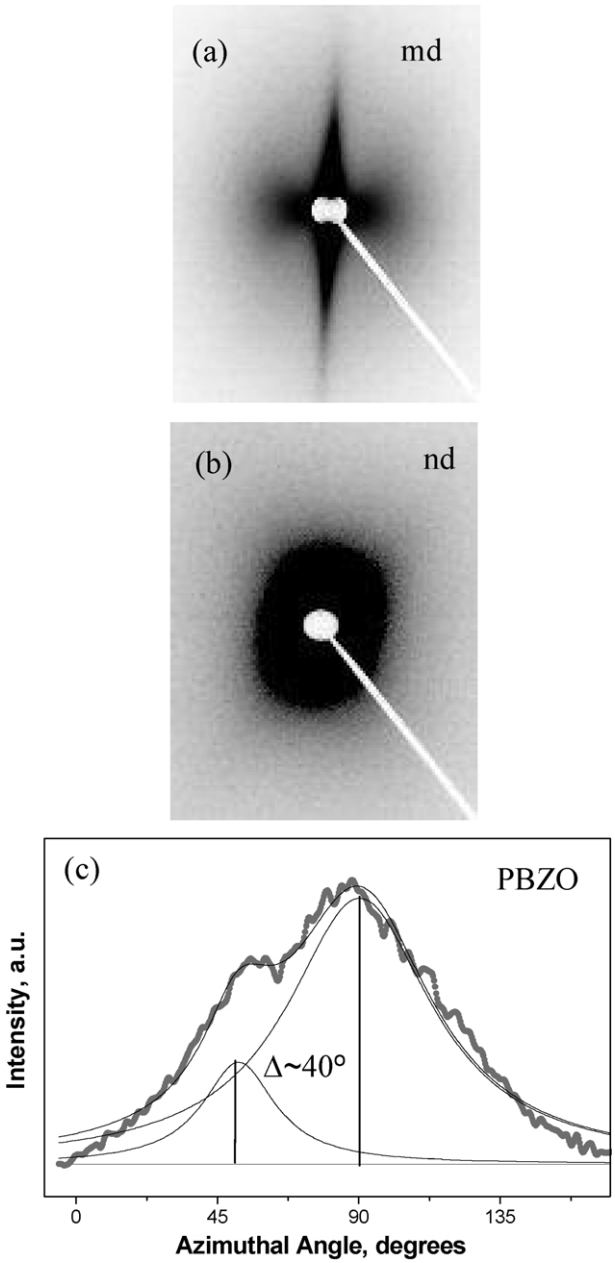

Fig. 14. (a) SAXS pattern with the X-ray beam parallel to the PBZO membrane surface, (b) pattern with the beam perpendicular to the surface, and (c) results (the darkest/widest/slightly irregular curve) of an azimuthal scan of the pattern in (b) at a 2θ value of 0.1 degree and resolution of the peak into its two constituents (the thinnest lines).

successive layers between the surface and the core. A progressive shift in angular direction was not observed. Fig. 12 exhibits a partial series of images progressing from the inside surface (as defined previously) of the membrane (top left) through the core to the outside surface (bottom right). The fibrils on the inside and outside are at ~ − 22 degrees and ~ + 22 degrees from the machine direction, respectively. The total angular separation based on 40 measurements is ~46 ± 3 degrees which is only slightly less than the value of 48 degrees determined by WAXD. The surface

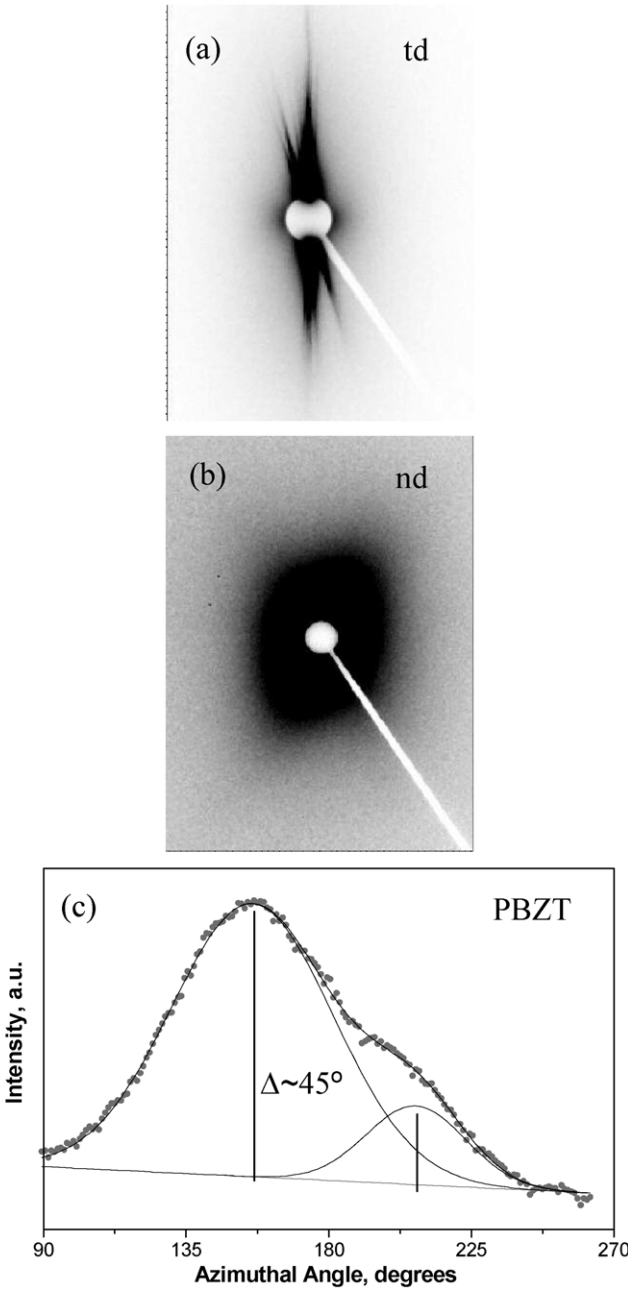

Fig. 15. (a) SAXS pattern with the X-ray beam parallel to the PBZT membrane surface, (b) pattern with the beam perpendicular to the surface, and (c) results (the darkest line with the data points) of an azimuthal scan of the pattern in (b) at a 2θ value of 0.1 degree and resolution of the peak into its two constituents (the thinnest lines).

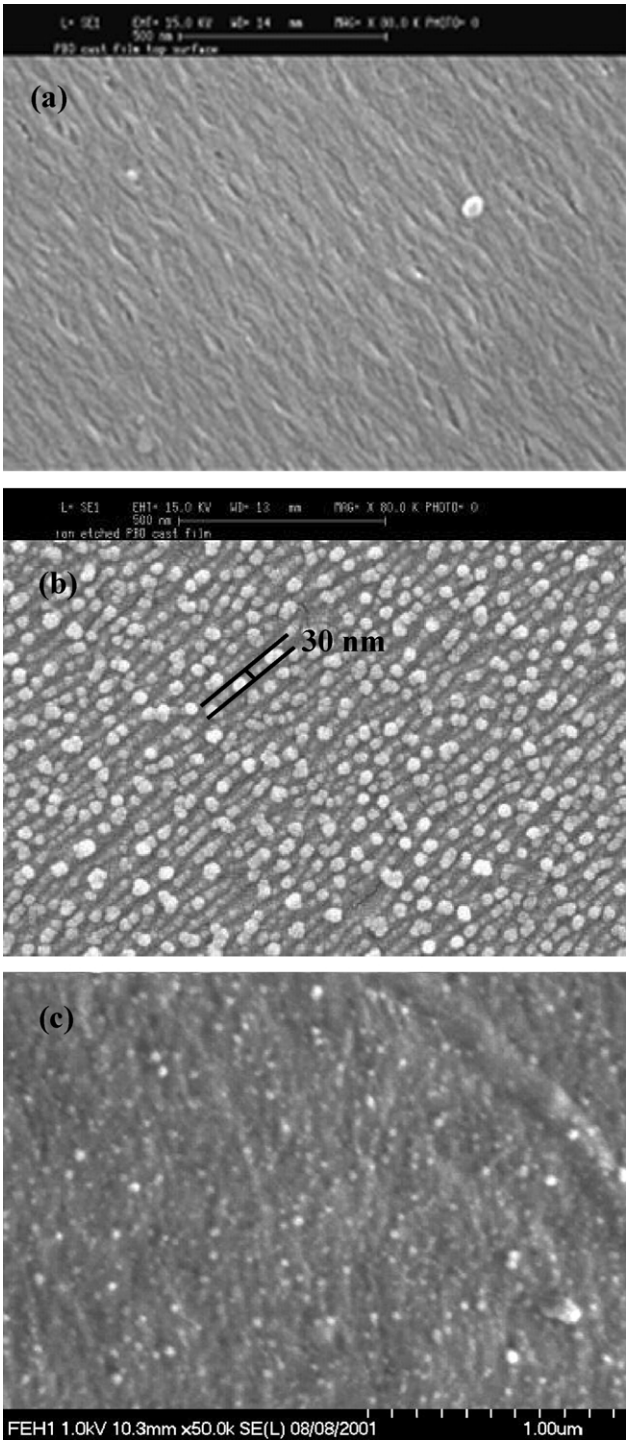

Fig. 16. SEM images of PBZO (a) before etching with plasma, (b) after etching with plasma, and (c) unetched but coated with sputtered carbon.

layers are each about 1 μm thick and the core is about 2.6 μm thick. Thus, the membrane is about 60% core.

3.3. SEM and SAXS of PBZO and SAXS of PBZT

Fig. 13(a) is an SEM image of a fractured cross section of the CRD-extruded PBZO membrane. The layered structures are typical of membranes made from rigid-rod polymers including PBZO, PBZT and others [12,15,18]. The layered structure has voids between the layers and those voids can also be sheet-shaped and parallel to the membrane surface. Fig. 13(b) shows a TEM image of the PBZO membrane microtomed perpendicular to the membrane surface. The layered structures akin to those in the fractured sample (Fig. 13(a)) are clearly seen and their thickness is in the range of 10–100 nm. Fig. 14(a) shows the SAXS pattern with the X-ray beam parallel to the surface of an unfractured PBZO

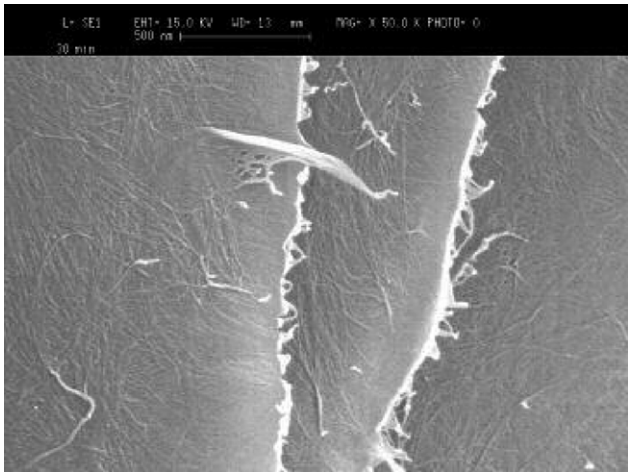

Fig. 17. SEM image of PBZO membrane cleaved surface made during plasma etching.

membrane (td). The scattering is elongated along the vertical direction, which is perpendicular to the membrane surface. The void structure gives anisotropic scattering as a result of the electron density difference between the layers and air, coupled with the thin extended shape of the voids. Fig. 14(b) shows the SAXS pattern with the beam perpendicular to the membrane surface (nd). If the pattern is scanned azimuthally at a value of 2θ of 0.1 degree, the darkest, widest, slightly irregular curve in Fig. 14(c) results. There is a non-uniform intensity distribution with a similar peak near 270 degrees (not shown). The peak associated exhibits a shoulder. Resolving the peak into its two constituents yields two peaks (the thinnest lines) near 50 and 90 degrees. The separation of about 40 degrees is close to the values obtained by WAXD (40) and AFM (44 ± 4). Probably this results from voids aligned parallel to the fibrils on the two surfaces of the membrane. Fig. 15 shows the corresponding SAXS results (a) and (b) for an unfractured PBZT membrane. In this case, the two peaks are separated by about 45 degrees (c) which again is close to the values obtained by WAXD (48) and AFM (46 ± 3). Fig. 16 shows SEM images of the PBZO membrane before (a) and after (b) etching with plasma. The membrane in Fig. 16(c) is unetched, but has been lightly coated with carbon by sputtering. Fibrils can be seen in all three images as well as ball-shaped unknown particles, in (b) and (c). Elemental analysis shows that these particles are not foreign material. They may have been made during plasma etching or carbon coating, although their origin is unknown. However, it is clear that there are fibrils. Additionally it was confirmed that the fibrils on the outside and inside surfaces are oriented in 'opposite' directions. These results are in harmony with the AFM, SAXS and WAXD results given above.

Fig. 17 is an SEM image of the PBZO membrane which happened to be cleaved during plasma etching. Thus, fibrils were observed on the surface of layers in the middle part of the membrane and were found to be randomly oriented with the width of fibrils being similar to those observed on the surface in Fig. 16. If the molecules are oriented along the fibrils, the direction of the molecular orientation in the middle part of the membrane is irregular while the molecules on the surfaces of the membrane are oriented along the shear direction. These results agree with those obtained by WAXD, AFM, and SAXS above. All the results are in contrast to the cholesteric morphology [12]. The cholesteric twist can easily be imagined because the molecular orientation of the top and bottom surface is minus theta to plus theta. However, the orientation developed by mechanical force during CRD extrusion is different from the cholesteric ordering in the liquid crystals developed by the molecular structure itself. The mechanical force would have to be transferred in the middle part of the membrane in order to have cholesteric orientation in the extruded membrane. If there were not much friction between molecules, it would be difficult to transfer the shear force from the top surface to the middle part of the membrane. Even if the shear force were transferred to the middle part of the membrane, the cholesteric orientation could be lost during coagulation if the molecular relaxation were fast enough. The existence of irregular order in the 60–70% of the membranes which is core suggests that the core of the polymer membrane probably contains voids to hold an ICP and to establish conducting channels. Further, the voids between the layers and the voids parallel to the fibrils present the possibilities for holding an ICP and establishing conducting channels.

4. Conclusions

The structures of CRD-extruded PBZO and PBZT membranes were studied using WAXD, SAXS, SEM, TEM, and AFM methods and compared with those for cast PBZO membrane. SEM, AFM, and TEM images show that the extruded membranes have sheet structures, typical of the rigid-rod polymers. The heterocyclic rings of the extruded membranes were oriented approximately parallel to the membrane surface, while those of the cast PBZO membranes were oriented perpendicular to the membrane surface. The parallel orientation of the heterocyclic rings of the extruded membranes may be due to the normal force exerted during extrusion. The polymer molecules in the region of the surfaces of the extruded membranes were oriented along the shear directions of extruder, although those in the middle sheet were oriented irregularly. The membranes exhibited little cholesteric nature. These kinds of orientation were confirmed with WAXD, SAXS, SEM, and AFM observations. The disordered core of the membranes together with the voids between the layers and the fibrils are consistent with the membranes being able to hold ICPs and establish conductive channels.

Acknowledgements

The work at the University of Akron was supported by WPAFB through a contract from the University of Dayton Research Institute. The PBZT membrane was provided by CS Wang of the University of Dayton Research Institute and the PBZO membrane by Foster–Miller, Inc. We thank T McCue and D Hull of the NASA Glenn Research Center for help with the SEM images. We thank F Yeh for help at the BNL beamline X27C. We thank A Sinsawat for help with the Cerius^2 program. Finally, we thank the reviewers for their helpful comments and suggestions.

References

[1] Blomen LJ, Mugerwa MN, editors. Fuel cell systems. New York: Plenum; 1994.
[2] Appleby AJ, Foulkes FR, editors. Fuel cell handbook. Malabar, FL: Krieger; 1993.
[3] Bessel S, Bronoel G, Tassin N, Naimi Y, Tounsi A. New materials for fuel cell systems I. Proceedings of international symposium on new materials for fuel cell systems I, Montreal; 1995.
[4] Amine K, Yasuda K, Takenaka H. Ann Chim Sci Mat 1998;23:331.
[5] Wolfe JF, Loo BH, Arnold FE. Macromolecules 1981;14:915.
[6] So YH. Prog Polym Sci 2000;25:137.
[7] Fratini AV, Lenhert PG, Resch TJ, Adams WW. Mater Res Soc Symp Proc 1989;134:431.
[8] Martin DC, Thomas EL. Macromolecules 1991;24:2450.
[9] Tashiro K, Yoshino J, Kitagawa T, Murase H, Yabuki K. Macromolecules 1998;31:5430.
[10] Takahashi Y, Sul H. J Polym Sci Part B: Polym Phys 2000;38:376.
[11] Jiang H, Eby RK, Adams WW. In: Kroschwitz J, editor. Encyclopedia of polymer science, 3rd ed. New York: Wiley; 2002.
[12] Tsabba Y, Rein DM, Cohen Y. J Polym Sci Part B: Polym Phys 2002; 40:1087.
[13] Lusignea RW. Mater Res Soc Symp Proc 1989;134:265.
[14] Hammersley AP. ESRF Internal Report, ESRF97HA02F, Fit2D: an introduction and overview, 1997; Hammersley AP, Svensson SO, Hanfland M, Fitch AN, Haeusermann D. Two-dimensional detector software: from real detector to idealised image or two-theta scan, High Pressure Research, vol. 14; 1996. p. 235.
[15] Song HH, Wang C-S. Polym Commun 1993;34:4793.
[16] Dean DR, Husband DM, Dotrong M, Wang C-S, Dotrong MH, Click WE, Evers RC. J Polym Sci Part A: Polym Chem 1997;35:3457.
[17] Song HH, Fratini AV, Chabinyc M, Price GE, Agrawal AK, Wang C-S, Burkette J, Dudis JS, Arnold FE. Synth Met 1995;69:533.
[18] Kim J, McHugh SK, Swager TM. Macromolecules 1999;32:1500.